

## Electronic Supporting Information

### Charge Stabilizing Tris(triphenylamine)-Zinc porphyrin-Carbon Nanotube

### Hybrids: Synthesis, Characterization and Excited State Charge Transfer Studies

Luis M. Arellano,<sup>a</sup> Myriam Barrejón,<sup>a</sup> Habtom B. Gozebe,<sup>b</sup> María J. Gómez-Escalonilla,<sup>a</sup> José Luis G. Fierro,<sup>c</sup> Francis D'Souza<sup>b,\*</sup> and Fernando Langa<sup>a,\*</sup>

<sup>a</sup> *Universidad de Castilla-La Mancha, Instituto de Nanociencia, Nanotecnología y Materiales Moleculares (INAMOL), 45071-Toledo, Spain. E-mail: Fernando.Langa@uclm.es*

<sup>b</sup> *Chemistry and Materials Science and Engineering, University of North Texas, 76203-5017 Denton, TX, USA. E-mail: [Francis.D'Souza@UNT.edu](mailto:Francis.D'Souza@UNT.edu)*

<sup>c</sup> *Instituto de Catálisis y Petroleoquímica, CSIC, Cantoblanco, 28049, Madrid, Spain. E-mail: [jlgfierro@icp.csic.es](mailto:jlgfierro@icp.csic.es)*

<b>Contents</b>	<b><u>Page</u></b>
1. Instrumentations	S3
2. Synthesis of reference compound <b>5</b>	S6
3. Figure S1. <sup>1</sup> H NMR spectrum of compound <b>5</b> .	S7
4. Figure S2. <sup>13</sup> C NMR spectrum of compound <b>5</b> .	S8
5. Figure S3. MALDI-MS spectrum of compound <b>5</b>	S9
6. Figure S4. Raman spectrum of hybrids <b>1-2</b> and <b>5</b>	S10
7. Figure S5. Raman spectrum of 2D-band	S11
8. Figures S6-S7. XPS data	S12
9. Figure S8 AFM image	S13
10. Figure S9. Molecular mechanic calculations	S14
11. Figure S10. NIR absorption spectra of <i>pristine</i> DWCNT and SWCNT	S15
12. Figure S11. Fluorescence spectrum of <b>5</b> and <i>f</i> -SWCNT <b>2</b> in THF	S16
13. Figure 12. Fluorescence spectrum of <b>5</b> and <i>f</i> -SWCNT <b>2</b> at 400 nm excitation	S17
14. Figure S13. Spectroelectrochemical study of oxidized (TPA) <sub>4</sub> ZnP	S18
15. Figure S14. Femtosecond transient absorption spectra of (TPA) <sub>3</sub> ZnP	S19
16. Table S1. Binding energies	S20
17. Table S2. XPS elemental composition	S21
18. References	S22

## Instrumentations

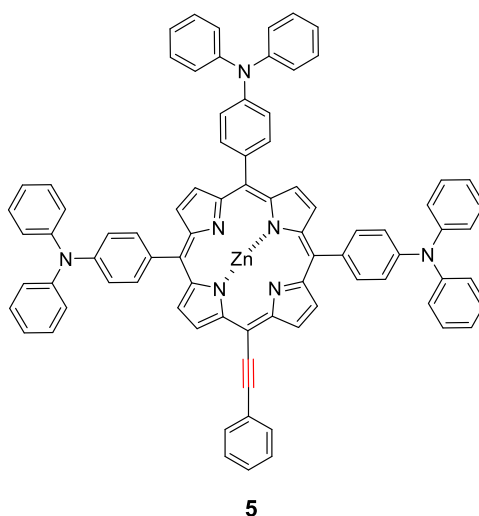
Sample sonication was carried out using an Elmasonic P 300 H sonicator bath (37 kHz). Microwaves reactions were performed in a CEM Discover reactor, equipped with fiber optic temperature detector and pressure control. Analytical thin layer chromatography (TLC) was performed using aluminium-coated Merck Kieselgel 60 F254 plates and flash chromatography was performed using silica gel (Scharlab 60, 230-240 mesh). NMR spectra were recorded on a Bruker Avance 400 ( $^1\text{H}$ : 400 MHz;  $^{13}\text{C}$ : 100 MHz) spectrometer at 298 K, unless otherwise stated, using partially deuterated solvents as internal standards. Coupling constants (J) are denoted in Hz and chemical shifts ( $\delta$ ) in ppm. Mass spectra (MALDI-TOF) were recorded on a VOYAGER DE<sup>TM</sup> STR mass spectrometer using dithranol as matrix. Thermogravimetric analyses (TGA) were performed using a TGA/DSC Linea Excellent instrument by Mettler-Toledo, collected under a flow of nitrogen (90 mLmin<sup>-1</sup>). The sample (~0.5 mg) was introduced inside a platinum crucible and equilibrated at 40 °C followed by a 10 °C/min ramp between 40 °C and 1000 °C. The weight changes were recorded as a function of temperature. UV/Vis spectra were recorded on a Shimadzu UV-VIS-NIR spectrophotometer UV-3600 in quartz cuvettes with a path length of 1 cm. The emission measurements were carried out on Cary Eclipse fluorescence spectrophotometer. Photoelectron spectra (XPS) were acquired with a VG Escalab 200R spectrometer equipped with a hemispherical electron analyser and a MgK $\alpha$  ( $h\nu = 1253.6$  eV,  $1$  eV =  $1.6302 \cdot 10^{-19}$  J) X-ray source, powered at 100 W. The kinetic energies of photoelectrons were measured using a hemispherical electron analyser working in the constant pass energy mode. The background pressure in the analysis chamber was maintained below  $8 \cdot 10^{-9}$  mbar during data acquisition. The XPS data signals were taken in increments of 0.1 eV with dwell times of 40 ms. Binding energies (BE) were calibrated relative to the C 1s peak at 284.8 eV. High resolution spectra envelopes were obtained by curve fitting synthetic peak components using the software -“XPS peak”-. The raw data were used with no preliminary smoothing. Symmetric Gaussian-Lorentzian (90%G-10%L) lines were used to

approximate the line shapes of the fitting components. Atomic ratios were computed from experimental intensity ratios and normalized by atomic sensitivity factors. Raman spectra were acquired with a Renishaw inVia Reflex Confocal Raman Microscope equipped with a 785 nm laser. Raman spectra were collected on numerous spots on the sample and recorded with a Peltier cooled CCD camera. Each sample was deposited as powder on a glass slide and was measured in multiple regions. The intensity ratio  $I_D/I_G$  was obtained by taking the peak intensities following any baseline corrections. The data were collected and analysed with Renishaw Wire and Origin software. Atomic force microscopy (AFM) images were obtained with a Multimode V8.10 (Veeco Instruments Inc., Santa Barbara, USA) with a NanoScope V controller (Digital Instruments, Santa Barbara, USA). The samples were prepared by drop casting onto a silicon wafer using a dispersion of the different samples in sodium dodecylbenzene sulfonate (NaDDBS). Cyclic voltammetry was performed in benzonitrile solution. Tetrabutylammonium hexafluorophosphate (0.1 M as supporting electrolyte) was purchased from Acros and used without purification. Solutions were deoxygenated by bubbling argon through prior to each experiment which was run under an argon atmosphere. Experiments were carried out in a one-compartment cell equipped with a platinum working microelectrode ( $\varnothing = 2$  mm) and a platinum wire counter electrode. An Ag/AgNO<sub>3</sub> electrode was used as reference and checked against the ferrocene/ferrocenium couple (Fc/Fc<sup>+</sup>) before and after each experiment.

Femtosecond transient absorption spectroscopy experiments were performed using an Ultrafast Femtosecond Laser Source (Libra) by Coherent incorporating diode-pumped, mode locked Ti:Sapphire laser (Vitesse) and a diode-pumped intra cavity doubled Nd:YLF laser (Evolution) to generate a compressed laser output of 1.45 W. For optical detection, a Helios transient absorption spectrometer coupled with femtosecond harmonics, generator both supplied by Ultrafast Systems LLC, was used. The source for the pump and probe pulses were derived from the fundamental output of Libra (Compressed output 1.45 W, pulse width 100 fs) at a repetition rate of 1 kHz. 95% of the fundamental output of the laser was introduced into a harmonic generator, which produces

second and third harmonics of 400 and 267 nm besides the fundamental 800 nm for excitation, while the rest of the output was used for the generation of white light continuum. In the present study, the second harmonic 400 nm excitation pump was used in all experiments. Kinetic traces at appropriate wavelengths were assembled from the time-resolved spectroscopic data. Data analysis was performed using Surface Xplorer software supplied by Ultrafast Systems. All measurements were conducted in degassed solutions at 298 K.

## Synthesis of [10,15,20-tri-(*N,N*-diphenylaniline)-5-ethynylphenyl]porphinato zinc(II) (**5**)



A 100 mL Schlenk flask was charged with  $\text{Pd}_2(\text{dba})_3$  (24.7 mg, 0.03 mmol) and  $\text{AsPh}_3$  (55.7 mg, 0.18 mmol). The flask was degassed and backfilled with argon for 1 hour. Subsequently, dry tetrahydrofuran (THF) (230 mL/mmol), unprotected porphyrin **3** (102 mg, 0.1 mmol), iodobenzene (0.10 mL, 0.27 mmol) and dry  $\text{Et}_3\text{N}$  (45 mL/mmol) were charged to the flask. The mixture was heated under reflux overnight. After cooling to room temperature, the organic solvent was removed under vacuum and the resulting crude product was purified by chromatography [silica gel hexane: AcOEt 95:5] and then precipitated with MeOH to afford the desired product **5** as a green solid (15 mg, 14% yield).  $^1\text{H}$  NMR ( $\text{CDCl}_3$ , 400 MHz):  $\delta$ /ppm: 9.81 (d,  $J = 4.3$  Hz, 2H), 9.10 (d,  $J = 4.3$  Hz, 2H), 9.06 (d,  $J = 4.3$  Hz, 4H), 8.06 (dd,  $J = 8.0, 4.2$  Hz, 8H), 7.66–7.32 (m, 31 H), 7.22–7.06 (m, 8H).  $^{13}\text{C}$ -NMR ( $\text{CDCl}_3$ , 75 MHz): 152.2, 150.7, 150.1, 147.9, 147.4, 147.4, 136.4, 136.2, 135.4, 135.3, 132.9, 132.2, 131.6, 130.8, 129.5, 128.7, 128.4, 124.8, 124.3, 122.8, 121.9, 121.3, 99.9, 96.1, 92.6. UV-vis (NMP)  $\lambda_{\text{max}}/\text{nm}$  ( $\log \epsilon$ ): 634 (4.98), 583 (4.65), 450 (5.87), 308 (5.51); MS ( $m/z$ ) (MALDI-TOF): calculated for  $\text{C}_{82}\text{H}_{55}\text{N}_7\text{Zn}$ : 1203.77; found ( $\text{M}^+$ ): 1203.09.

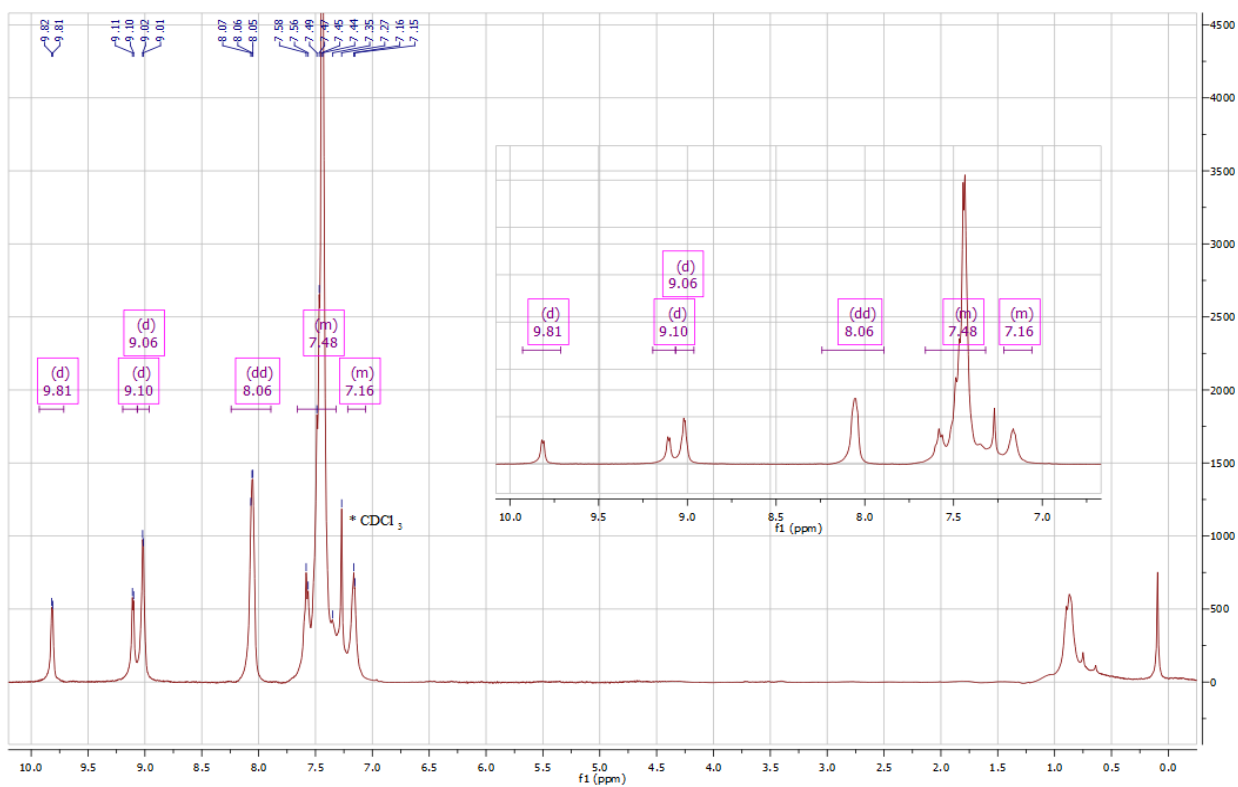


**Figure S1.**  $^1\text{H}$  NMR spectrum (400 MHz,  $\text{CDCl}_3$ ) of compound **5**.

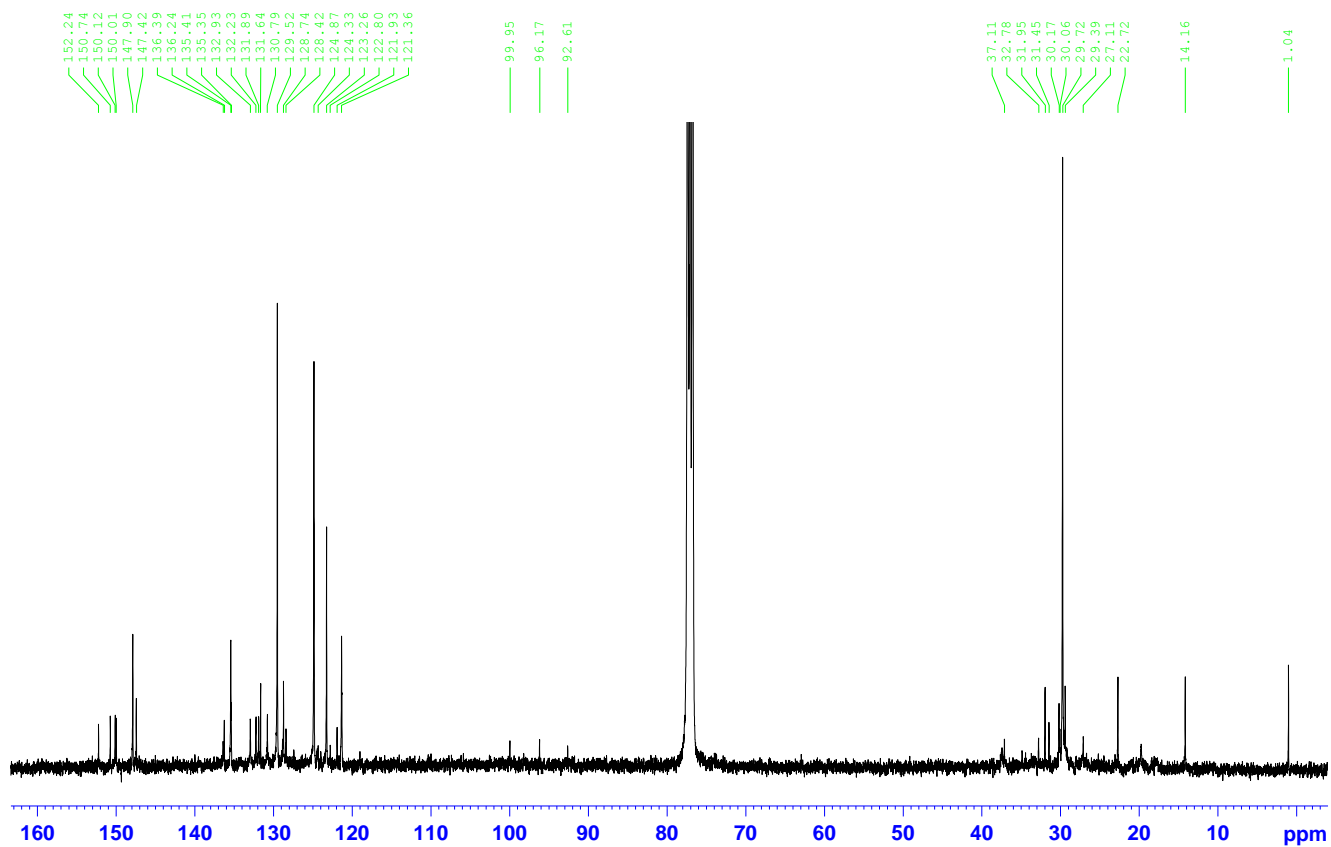


**Figure S2.**  $^{13}\text{C}$  NMR spectrum (100 MHz,  $\text{CDCl}_3$ ) of compound **5**.

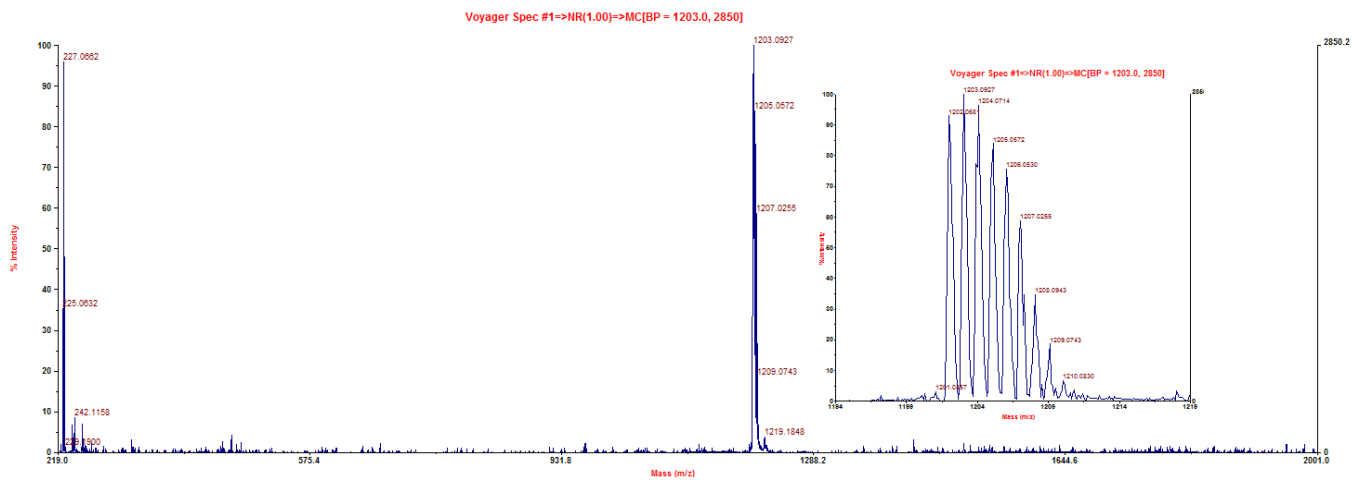
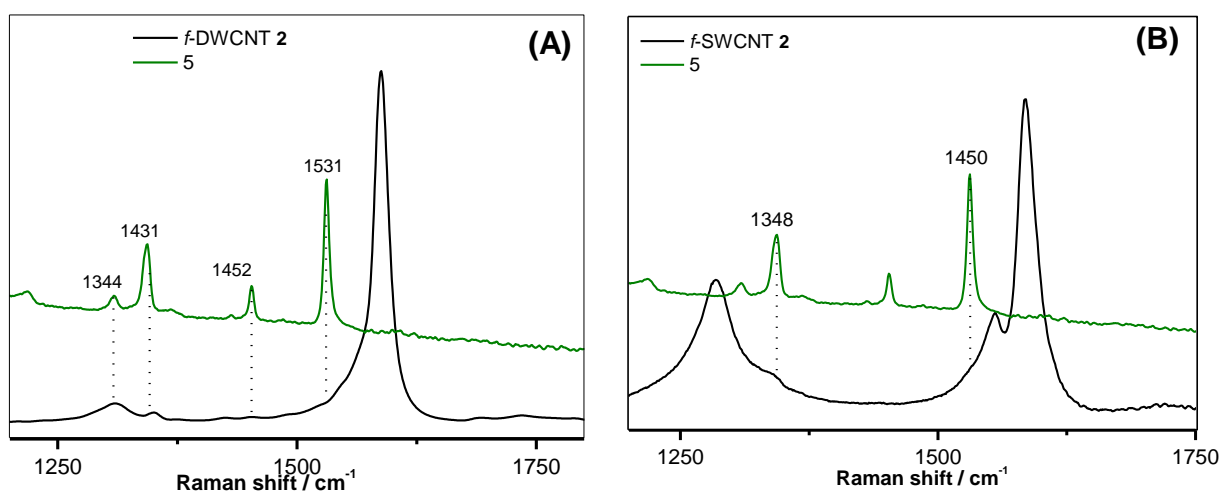
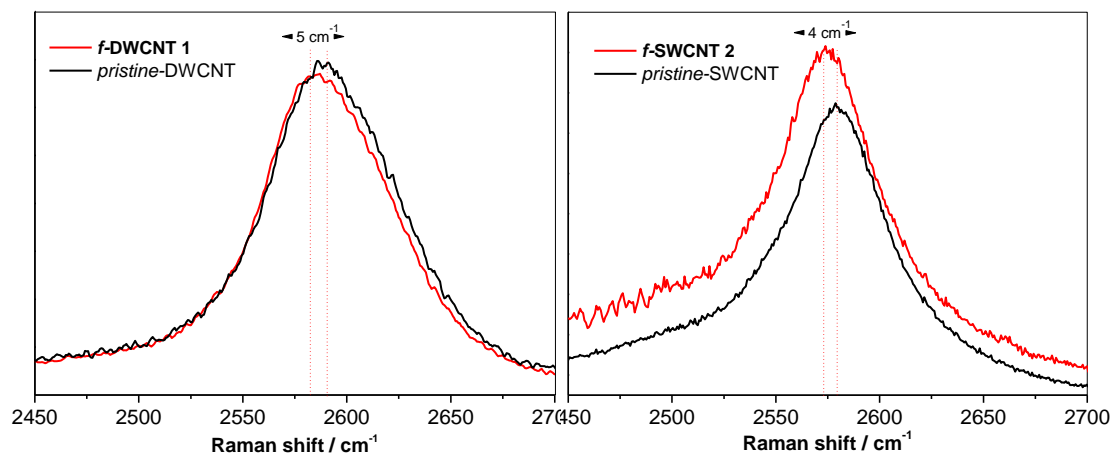


Figure S3. MALDI-MS spectrum of compound **5** (Matrix: Ditranol).



**Figure S4.** Raman spectrum (785 nm) of hybrids **1** (a) and **2** (b) comparing with precursor porphyrin **5**, showing the presence of bands attributed to the porphyrin moiety in nanoconjugates **1** and **2**.



**Figure S5.** Comparison of 2D-band of (left) *pristine* DWCNT and nanohybrid **1** and (right) *pristine* SWCNT and nanohybrid **2** upon 785 nm excitation.

The C 1s and O 1s core-level spectra of the *pristine* DWCNT and SWCNT samples are shown in Figures S6 and S7, respectively. Following the assignment by Stankovich<sup>1</sup> and our previous works,<sup>2</sup> the C 1s emission was satisfactorily curve-resolved with five components: the most intense peak, at 284.8 eV, is assigned to sp<sup>2</sup> C-atoms of the graphene structure. This peak, together with the weak  $\pi$ - $\pi^*$  plasmon component at about 291.3 eV, is indicative of the graphene structure in both DWCNT and SWCNT (see Figure S6). The component at 286.3 eV is often assigned to C–OH, and the components at 287.7 and 289.2 eV to C=O and –COO– species, respectively.<sup>3</sup> Similarly, the O 1s line was curve-resolved with two components (Figure S7). The minor component at around 532 eV corresponds to O=C surface groups whereas the major one at around 533 eV is often associated with the O–C bond.

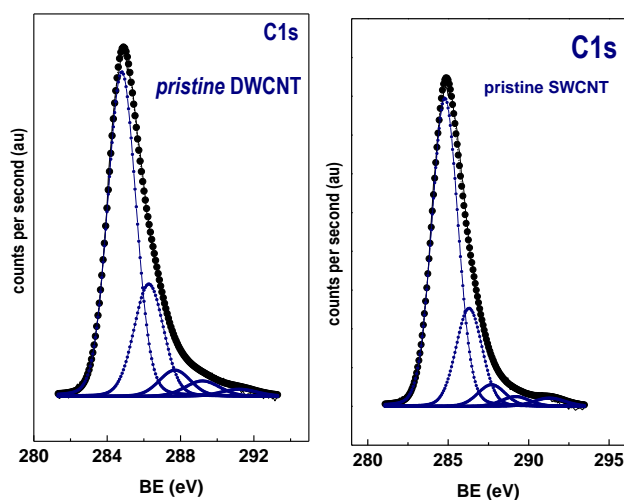


**Figure S6.** C1s XPS spectra of *pristine* DWCNT and SWCNT.

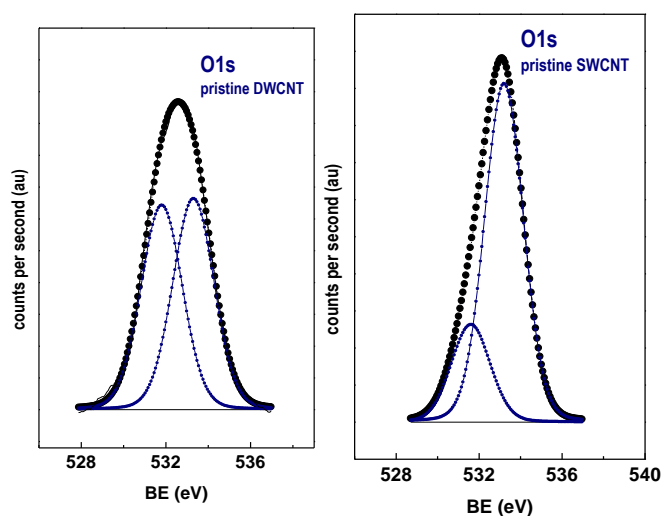


**Figure S7.** O1s XPS spectra of *pristine* DWCNT and SWCNT

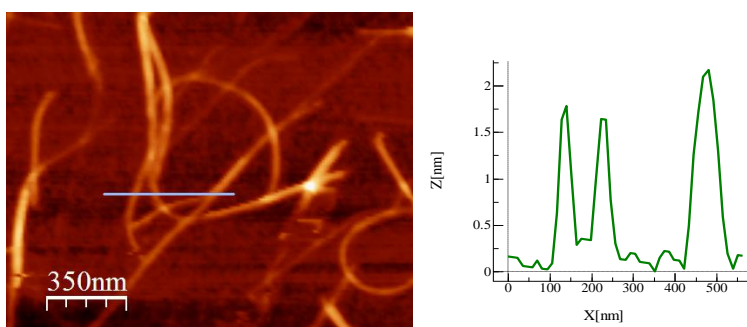


**Figure S8.** AFM images and height profile along the region indicated for *pristine* DWCNT showing the diameter distribution of the sample.

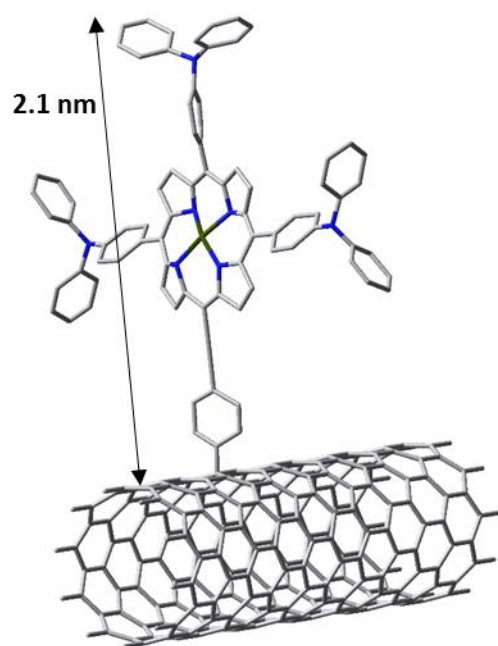


**Figure S9.** Modelling structures optimized using semiempirical PM3 method implemented on HyperChem 8.0 program package.

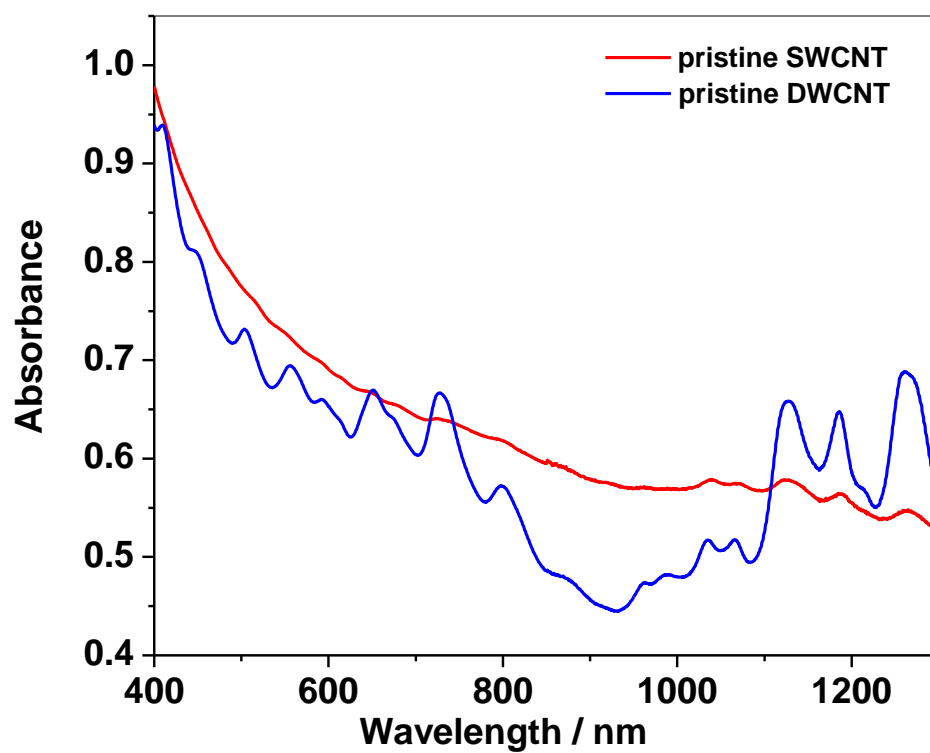


**Figure S10.** NIR absorption spectra of *pristine* CNTs in aqueous sodium cholate hydrate.

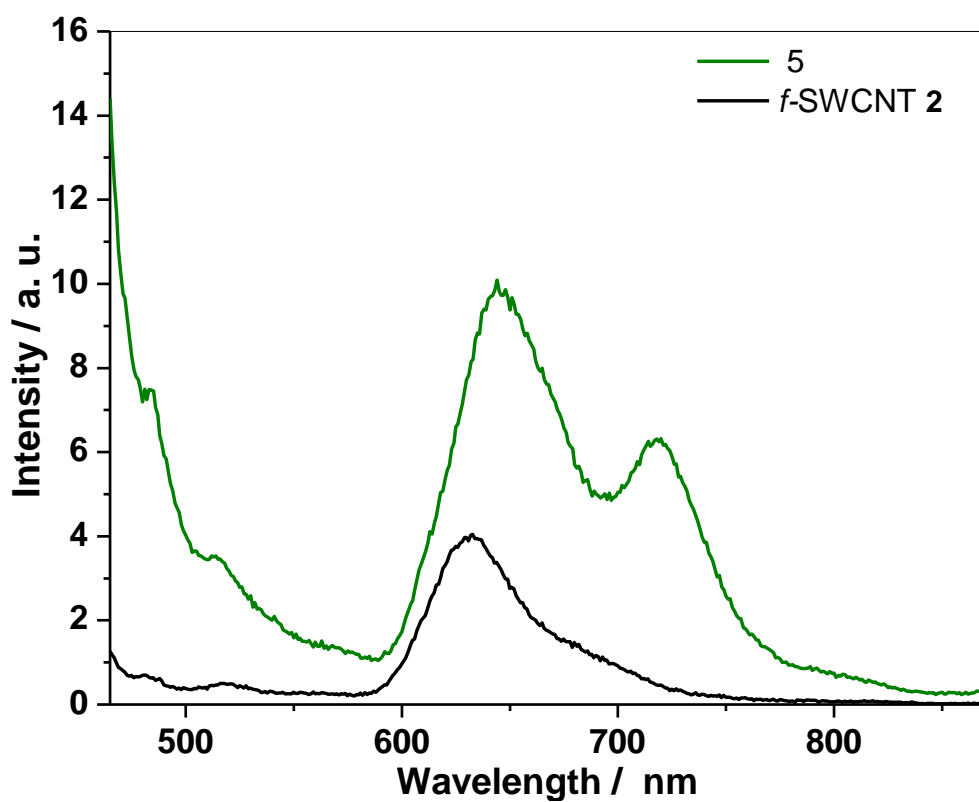


**Figure S11.** Fluorescence spectra of *f*-SWCNT **2** (black line) and reference porphyrin **5** (green line) in tetrahydrofuran (THF) with dispersions exhibiting the same optical absorption ( $\lambda_{\text{exc}} = 442$  nm).

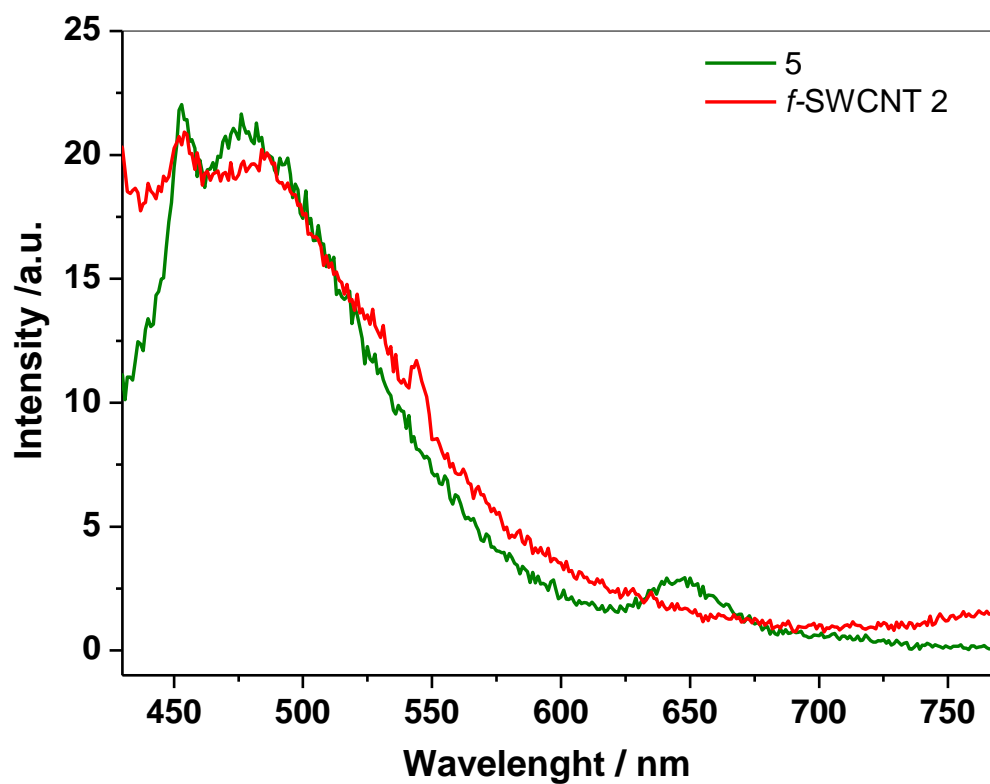


**Figure S12.** Fluorescence spectra of *f*-SWCNT **2** (red line) and reference porphyrin **5** (green line) in NMP with dispersions exhibiting the same optical absorption ( $\lambda_{\text{exc}} = 400 \text{ nm}$ ).

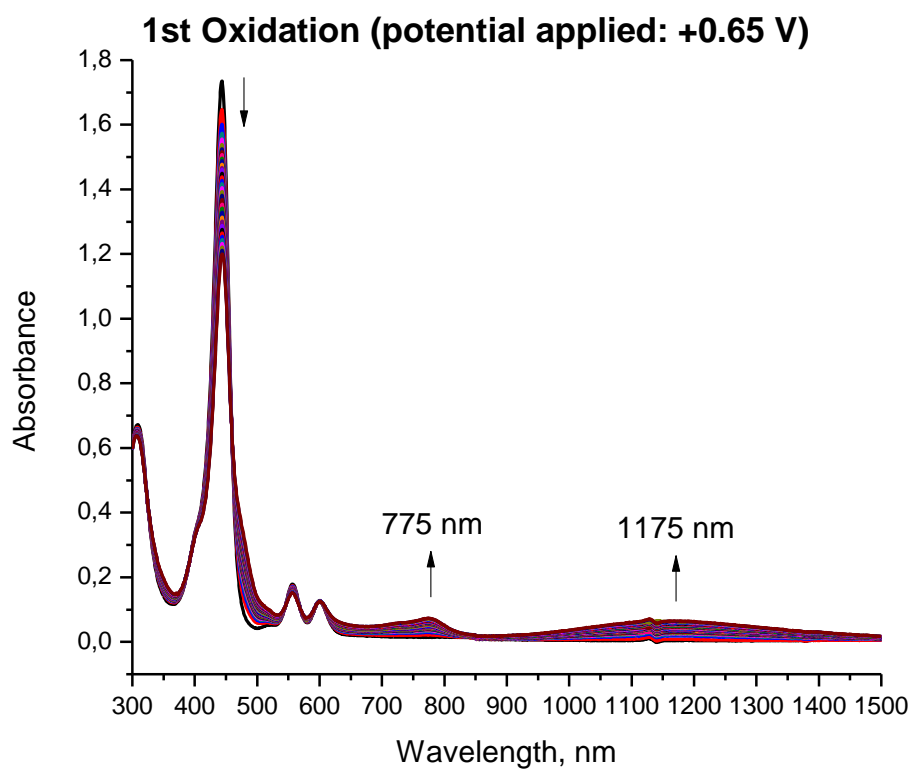


**Figure S13.** Spectroelectrochemical study of oxidized (TPA)<sub>4</sub>ZnP; ( $E_{\text{applied}} = 0.65$  V vs. Ag/AgCl).

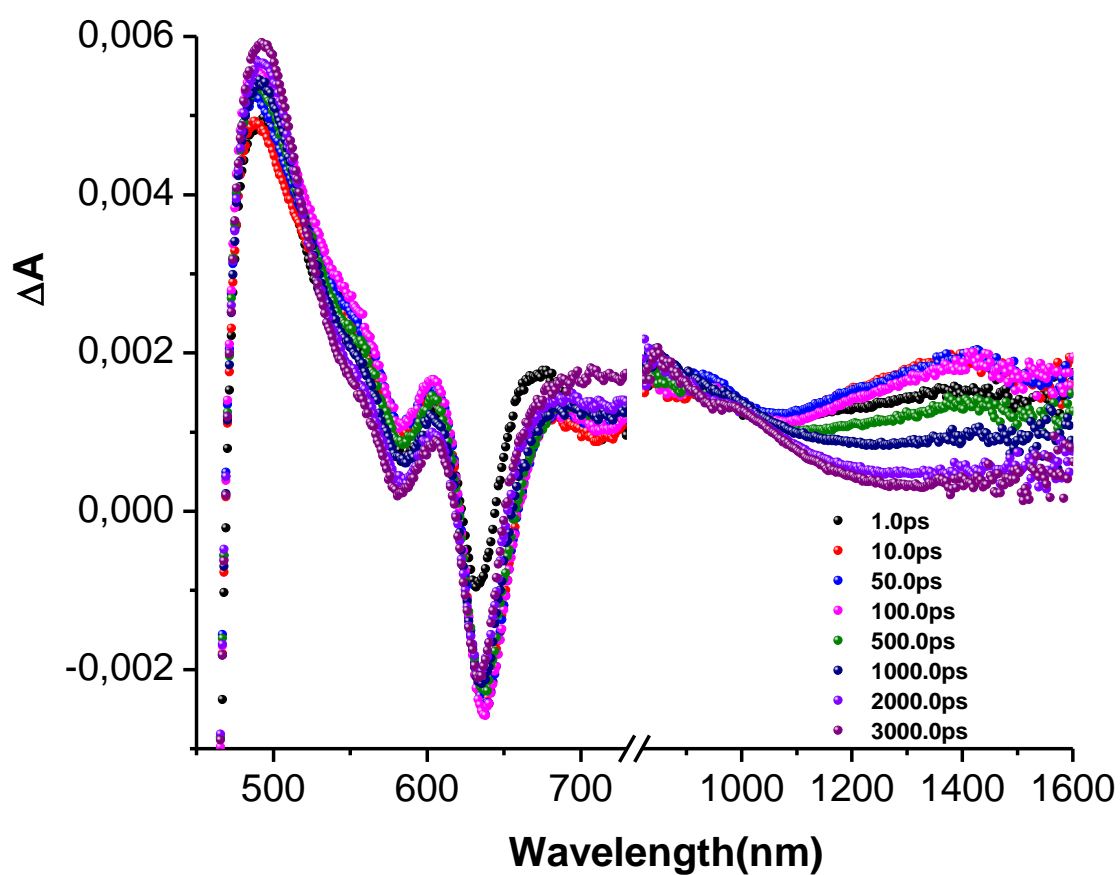


**Figure S14.** Femtosecond transient absorption spectra of the porphyrin reference compound **5**,  $(\text{TPA})_3\text{ZnP}$  in NMP.

**Table S1.** Binding energy (eV) of the core-level atoms of *functionalized* samples and its precursors. The peak percentages are indicated in brackets.

Sample	C1s BE (eV)						O1s BE (eV)		N1s BE (eV)		Si2p BE (eV)	Zn2p <sub>3/2</sub> BE (eV)	I3d <sub>5/2</sub> BE (eV)
	sp <sup>2</sup> C	sp <sup>3</sup> C	C-O	C=O	COO	$\pi$ - $\pi^*$	O=C	O-C	=N-	NH-			
<i>pristine-SWCNT</i>	284.8 (69)		286.3 (22)	287.7 (5)	289.2 (4)	291.3 (2)	531.6 (27)	533.2 (73)					
<i>pristine-DWCNT</i>	284.8 (69)		286.2 (16)	287.7 (6)	289.2 (4)	291.3 (5)	531.8 (49)	533.3 (51)					
<b>SWCNT-I</b>	284.8 (63)		286.2 (24)	287.7 (9)	289.2 (4)		532.0 (30)	533.4 (70)			101.3		620.6
<b>DWCNT-I</b>	284.8 (58)		286.1 (28)	287.5 (9)	289.4 (5)		531.6 (27)	533.3 (73)					621.2
<b>ZnPTPA-TMS (4)</b>	284.8 (82) 286.4 (18)								398.5 (43)	400.1 (57)	102.3	1021.9	
<i>f</i> -SWCNT 2	284.8 (68)		286.2 (27)	288.1 (5)			532.1 (38)	533.4 (62)	399.1 (43)	400.1 (57)		1021.7	620.7
<i>f</i> -DWCNT 1	284.8 (63)		286.3 (24)	288.0 (13)			532.1 (29)	533.4 (71)	398.8 (43)	400.7 (57)	103.8	1022.0	621.2

**Table S2:** XPS elemental composition of *pristine* SWCNT and DWCNT, *functionalized* samples and its precursors.

Sample	C (%at)	O (%at)	N (%at)	Si (%at)	Zn (%at)	I (%at)
(TPA) <sub>3</sub> ZnP-TMS ( <b>4</b> )	98.3	-	1.3	-	0.2	0.2
<i>pristine</i> <b>SWCNT</b>	95.7	4.3	-	-	-	-
<i>pristine</i> <b>DWCNT</b>	95.1	4.9	-	-	-	-
SWCNT-I	93.7	4.3	-	-	-	2.0
DWCNT-I	94.1	5.0	-	-	-	0.9
<i>f</i> -SWCNT <b>2</b>	93.3	5.2	1.0	-	0.2	0.3
<i>f</i> -DWCNT <b>1</b>	93.4	5.0	1.2	-	0.2	0.2

References:

---

<sup>1</sup> S. Stankovich, D. A. Dikin, R. D. Piner, K. A. Kohlhaas, A. Kleinhammes, Y. Jia, Y. Wu, S. T. Nguyen and R. S. Ruoff, *Carbon*, **2007**, *45*, 1558-1565.

<sup>2</sup> (a) M. Barrejon, S. Pla, I. Berlanga, M. J. Gómez-Escalonilla, L. Martín-Gomis, J. L. G. Fierro, M. Zhang, M. Yudasaka, S. Iijima, H. B. Gobeze, F. D'Souza, Á. Sastre-Santos and F. Langa, *J. Mater. Chem. C*, **2015**, *3*, 4960-4969; (b) M. Vizuite, M. J. Gómez-Escalonilla, J. L. G. Fierro, P. Atienzar, H. García and F. Langa, *ChemPhysChem*, **2014**, *15*, 100-108.

<sup>3</sup> (a) H. P. Boehm, *Carbon*, **2002**, *40*, 145-149; (b) A. Criado, M. Vizuite, M. J. Gómez-Escalonilla, S. García-Rodríguez, J. L. G. Fierro, A. Cobas, D. Peña, E. Guitián and F. Langa, *Carbon*, **2013**, *63*, 140-148.